EurJIC European Journal of Inorganic Chemistry

FULL PAPER

DOI: 10.1002/ejic.201200695

Functional Hybrid Materials Based on Layered Simple Hydroxide Hosts and Dicarboxylate Schiff Base Metal Complex Guests

Séraphin Eyele-Mezui,[a] Emilie Delahaye,[a][‡] Guillaume Rogez,*[a] and Pierre Rabu*[a]

Keywords: Hybrid materials / Layered compounds / Schiff bases / Magnetic properties / Hydroxides

The insertion of carboxysalen-type complexes into magnetic layered transition-metal simple hydroxides has provided new hybrid compounds. Three kinds of carboxysalen ligands have been used: an ethylenediamine bridge (SED-H_2), a chiral cyclohexanediamine bridge [(*S*,*S*)-SCD-H_2 and (*R*,*R*)-SCD-H_2], and an aromatic *o*-phenylenediamine bridge (SBD-H_2). The ccorresponding Cu^{II}, Ni^{II}, Co^{II}, Zn^{II}, Mn^{III}, and Al^{III} complexes were synthesized and inserted into layered cobalt and copper hydroxides. The structural and spectroscopic investigations confirmed the successful insertion-grafting of the complexes leading to new layered hybrid materials in which the inserted complexes act as pillars between the inorganic layers. The use of carboxylate anchoring functions enabled some of the difficulties encountered during the previously reported insertion of sulfonatosalen complex analogues to be overcome, namely hydrolysis and decomplexation during the insertion reaction. Hence, in this work it was possible to insert a wide variety of complexes into layered simple hydroxides, including M^{III} complexes, for the first time. The insertion of chiral carboxysalen complexes led to the formation of chiral magnets in which chirality transfer to the inorganic layers was evidenced and seems to be favored by the carboxylate anchoring groups. Finally, magnetic characterization showed that the copper hydroxide hybrids exhibit overall antiferrimagnetic behavior, whereas the cobalt hydroxide hybrids present ferromagnetic ordering, with ordering temperatures ranging from 6.5 to 12.8 K. In this case the nature of the cation inserted between the layers influences the magnetic behavior of the hybrid, contrary to what was observed in the case of the sulfonate analogues.

Introduction

Nowadays, the controlled synthesis of hybrid materials is of particular interest for the design of new materials with specific chemical, physical, or biological properties.[1–13] For example, the insertion of organic or organometallic species into layered inorganic compounds can lead to original nanosized organic/inorganic, inorganic/inorganic, or bio/inorganic functional heterostructures.[14–30] Through the multiscale organization of their components and because of synergistic effects, such materials can acquire new properties not found elsewhere and become “multi-materials”, that is, unique materials that simultaneously meet several requirements. Layered systems, in which the properties of each sub-network and their synergy can be tuned by the topology and chemical bonding between constituents, have been found to exhibit striking combinations of properties, such as magneto-optical, photomagnetic, or magnetic and supraconductive. Chemistry plays a major role in improving the interactions between organic and inorganic networks, and it is essential to identify and control the structural features and physical mechanisms influencing the properties of these new hierarchically organized nanostructures.[13]

In recent work devoted to the methodical investigation of hybrid organic/inorganic magnetic compounds and their functionalization,[19] the special case of the insertion by anion exchange of Schiff base disulfonates $[M\{salen(SO_3)_2\}]^{2-}$ and $[M\{(R,R)$- or (S,S)-$Cysalen(SO_3)_2\}]^{2-}$ ($M = Cu^{2+}, Ni^{2+}, Co^{2+}$, and Zn^{2+}) into copper(II) and cobalt(II) hydroxides, $[Cu_2(OH)_3(DS)]$ and $[Co_2(OH)_3(DS_0)]$ ($DS^- =$ dodecyl sulfate and $DS_0^- =$ dodecyl sulfonate), was reported.[31,32]

The structures of these compounds were established by the combined use of X-ray powder diffraction (XRPD), elemental analysis, FTIR and UV/Vis spectroscopy, and X-ray photoelectron spectroscopy (XPS). Treatment of the starting hydroxides with a solution of the nickel Schiff bases $[Ni\{salen(SO_3)_2\}]^{2-}$ and $[Ni\{(R,R)$- or (S,S)-$Cysalen(SO_3)_2\}]^{2-}$ led to the substitution of the alkyl anions by the nickel complexes retaining the structures of the parent hydroxide layers.[31] We showed that the chirality of the Ni–Cysalendisulfonates could be transferred to the whole hybrid structure to obtain a chiral magnet by design. This approach is very promising for the construction of new

---

[a] IPCMS, UMR CNRS-UdS 7504,
23 rue du Loess, B. P. 43, 67034 Strasbourg Cedex 2, France
Fax: +33-3-88107247
E-mail: rogez@ipcms.u-strasbg.fr
rabu@ipcms.u-strasbg.fr
Homepage: http://www-ipcms.u-strasbg.fr/spip.php?article422
[‡] Current address: Institut de Chimie Moléculaire et des Matériaux
d’Orsay, CNRS, Université Paris Sud 11,
91405 Orsay, France

Supporting information for this article is available on the WWW under http://dx.doi.org/10.1002/ejic.201200695.

multifunctional layered compounds. The Schiff base metal complexes are particularly appealing to this end, because such complexes can be used in electroluminescent devices,[33–35] nonlinear optics,[36–40] electrochemical sensors,[41,42] enantiocatalysis,[43,44] or as heterogeneous catalysts immobilized on polymers,[45] porous matrices,[46] or layered double hydroxides (LDHs).[47] In fact, we started to generalize this approach by using salen- and Cysalensulfonates of other metals.[32] However, the exchange reactions were not as straightforward as for the nickel complexes. We succeeded in inserting and grafting some Cu^{2+}, Ni^{2+}, Co^{2+}, and Zn^{2+} disulfonate complexes but, in some cases, cation exchange took place. Partial decomplexation was observed with exchange between the cations released by the complexes and the cations of the hydroxide layers. In the copper hydroxide analogues, such additional cation exchange led to the transformation of the single octahedral Cu^{II} layers into heterometallic triple-decker layers in the final products, as depicted in Scheme 1.

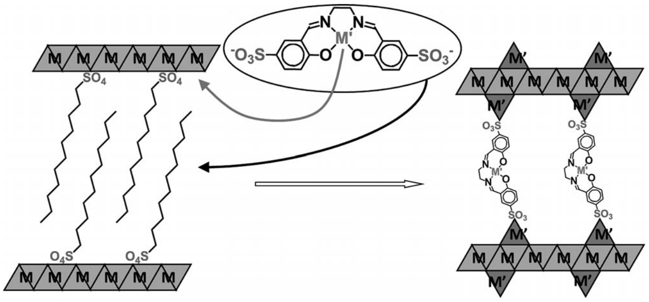

Scheme 1. Insertion-grafting of disulfonatosalen-type complexes into copper- and cobalt-layered hydroxides leads to drastic modification of the structures and compositions of the inorganic layers.

This phenomenon has been ascribed to the destabilization of the metal Schiff bases due to the presence of the sulfonate groups combined with the effect of the slightly alkaline character of the aqueous reaction medium.

Following these reports, this paper is intended first to outline the synthesis and structures of two homologous series of copper and cobalt hydroxides functionalized with transition-metal salen- and Cysalendicarboxylates, complexed by Cu^{2+}, Ni^{2+}, Co^{2+}, Zn^{2+}, Mn^{3+}, and Al^{3+}, and then to discuss their properties and finally make a comparison with the disulfonate analogues. The influence of the anchoring moieties, sulfonate or carboxylate, on the stabilities of the complexes during the functionalization process and on the magnetic properties is emphasized. In this respect, the results presented herein may be of broader significance, leading to a better interpretation of the properties of organic/inorganic functional materials derived from transition-metal-based matrices incorporating functional molecular hosts.

Results and Discussion

Synthesis of the Schiff Base Complexes

We synthesized a series of salen-type Schiff base dicarboxylate complexes in which the transition-metal ions lie in the ONNO planar coordination site (Figure 1). The carboxylate moieties are borne by the aromatic rings. The diamino bridges are simple ethylenediamine, chiral cyclohexanediamine, or the conjugated phenylenediamine.

The Schiff base ligands were synthesized by using modified literature procedures (see the Exp. Sect.)[48–54] by the condensation of 2 equiv. of 3-formyl-4-hydroxybenzoic acid (FBA-H)[48] with 1 equiv. of the corresponding diamine (1,2-diaminoethane, 1,2-diaminobenzene, or chiral 1,2-diaminocyclohexane[52–54]).

The SED-H_2 Schiff base ligand is only partially soluble in polar solvents such as DMSO or DMF and insoluble in alcohols and water. The dissolution of SED-H_2 in an alkaline aqueous solution followed by complexation did not give satisfactory results, except in the case of the complexation of Ni^{II}. In the other cases we observed the formation of hydroxides or oxides, and/or the hydrolysis of the ligand. Therefore, for the complexation of the Cu^{II}, Co^{II}, and Zn^{II} metal ions, the ligand was partially solubilized in DMF[50] before the addition of the corresponding metal acetate salt. The desired complexes were collected after precipitation with methanol. The Fe^{III} complex was synthesized by another procedure,[55] namely by heating a suspension of

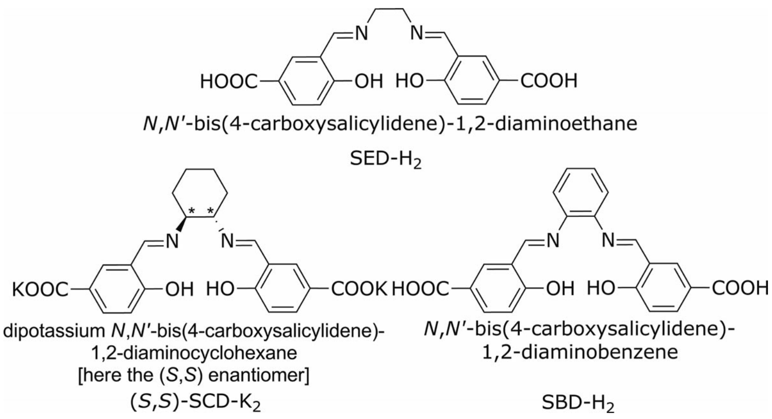

Figure 1. The salen-type Schiff bases used in this study (the nomenclature chosen indicates the protonation state of the carboxylate in the as-synthesized ligands).

SED-H_2 in dry ethanol at reflux with 2 equiv. of triethylamine and adding anhydrous $FeCl_3$ dissolved in dry ethanol. Finally, the Mn^{III} complex, SED-H_2–MnCl was synthesized by heating SED-H_2 and $Mn(OAc)_2{\cdot}4H_2O$ in methanol at reflux with an excess of LiCl. Mn^{II} was oxidized to Mn^{III} in air, characterized by a change in color from yellow-green to brown.

The potassium salt of the as-synthesized chiral ligand, SCD-K_2, is soluble in both water and methanol. Therefore, its complexation was easily performed by the addition of an aqueous solution of the metal acetate salt (Co and Mn) to a methanol solution of the ligand. The Mn^{III} compound was obtained upon oxidation in air in the presence of an excess of LiCl.

SBD-H_2 was complexed to Co^{II} in DMF and to Mn^{III} in methanol (with an excess of LiCl). The Al^{III} complex, SBD-H_2–AlCl, was synthesized in ethanol under argon by the reaction of SBD-H_2 with $Al(Et)_2Cl$.

Synthesis of the Hybrid Compounds

All the compounds were obtained by anion-exchange reactions starting from the cobalt or copper transition-metal layered simple hydroxides prefunctionalized with dodecyl sulfonate (DS_0^-) or dodecyl sulfate (DS^-), respectively (see the Exp. Sect.). The formation of the intermediates $[Co_2(OH)_3(DS_0)]$ and $[Cu_2(OH)_3(DS)]$ led to an increase in the interlamellar spacing (from 12.7 and 9.4 Å for $[Co_2(OH)_3(OAc)]{\cdot}H_2O$ and $[Cu_2(OH)_3(OAc)]{\cdot}H_2O$, respectively, to 25.1 and 26.7 Å for $[Co_2(OH)_3(DS_0)]$ and $[Cu_2(OH)_3(DS)]$, respectively). This increase allows for easier insertion-grafting of large molecules.[56] In addition, the grafting of long alkyl chains within the interlamellar space creates a local hydrophobic environment, which limits the hydrolysis of the complexes being inserted.[31,32] The final exchange reaction of the alkyl chains by the salencarboxylate complexes took place in 1:1 water/ethanol, which favored the solvation of the dodecyl sulfonate or dodecyl sulfate when removed from the interlamellar space. Finally, the temperature of the reaction was also an important parameter. All the reactions took place at reflux (around 80 °C). This temperature guaranteed the stability of the Schiff base complexes during the anion-exchange reactions and at the same time favored an efficient substitution rate with complete removal of the dodecyl sulfonate or dodecyl sulfate anions from the interlamellar space of the parent hydroxides. In the case of the functionalization of copper hydroxide, it was possible to proceed at a lower temperature (60 °C), but in this case the reactions took much longer (typically 24 h), and the crystallinity of the hybrids was not as good.

Most of the reactions were successful, yet all attempts to insert/graft the SED-H_2–Zn complex into cobalt hydroxide led to mixtures of nonlamellar compounds. The insertion of the SBD–AlCl complex into copper hydroxide led to the formation of $[Cu_2(OH)_3Cl]$. The insertion of the SED-H_2–FeCl complex into both cobalt and copper hydroxides led to lamellar compounds for which the elemental analysis showed a clear excess of Fe. Mössbauer spectroscopy did not allow determination of the precise structures of the compounds, which are still under investigation.

Structures of the Hybrid Compounds

All the compounds were characterized by ancillary techniques, powder X-ray diffraction, elemental analysis, TGA/TDA, FTIR, and UV spectroscopy.

The powder X-ray diffraction patterns of the starting compounds and of the hybrid derivatives are shown in Figures 2 and 3 for the cobalt and copper hydroxide derivatives, respectively.

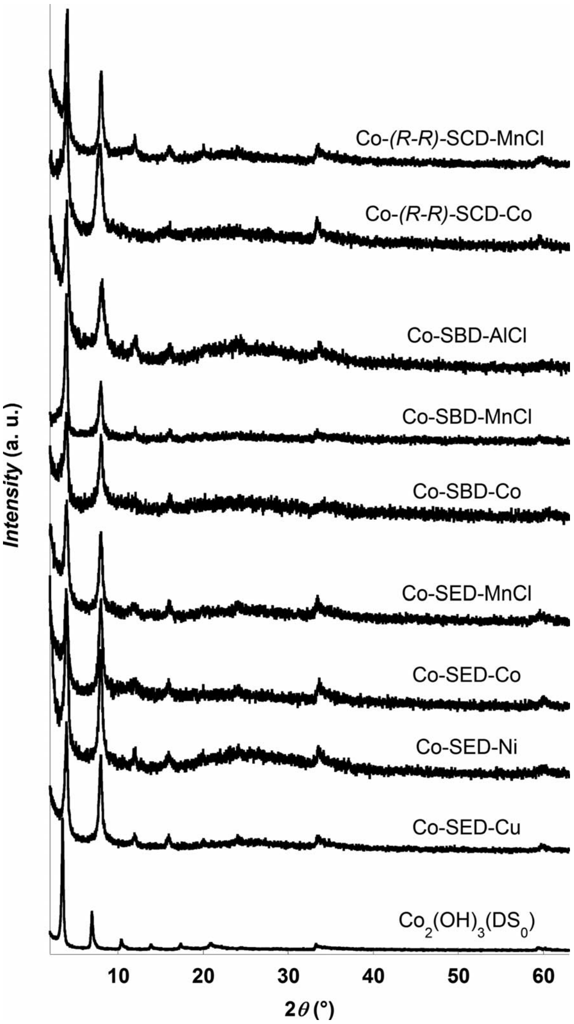

Figure 2. Powder XRD patterns of the hybrid compounds based on cobalt hydroxide (Cu-$K_{\alpha1}$ = 1.540598 Å).

In the low 2θ range ($2\theta < 35°$), the diffraction patterns of all the compounds show intense $00l$ diffraction lines up to at least the third harmonic, which evidences their lam-

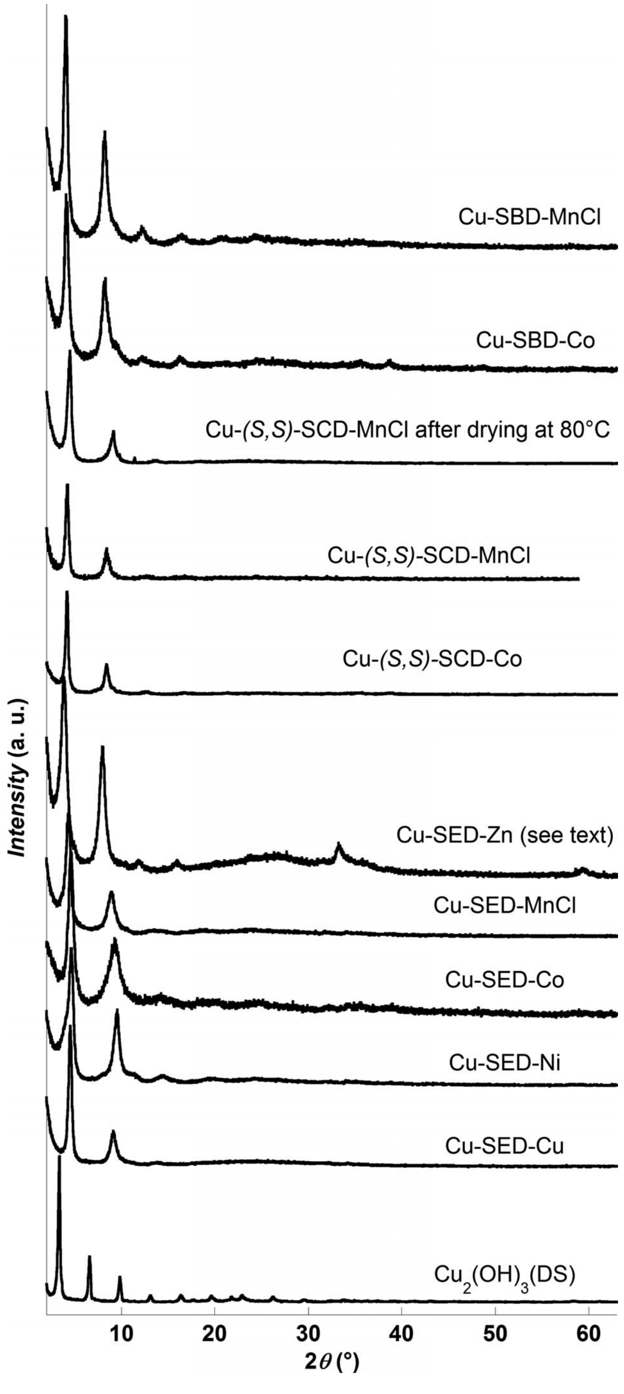

Figure 3. Powder XRD patterns of the hybrid compounds based on copper hydroxide (Cu-$K_{\alpha 1}$ = 1.540598 Å).

ellar structure. The experimental basal distances are collected in Table 1. All the compounds exhibit a marked shift of the 00*l* peak positions in comparison with the starting materials.

The XRD patterns of all the cobalt derivatives, including the starting compound [$Co_2(OH)_3(DS)$], exhibit similar features in the region of the in-plane diffraction lines (high 2θ angles) with characteristic asymmetrical peaks at 2θ = 33 and 60° (Cu-$K_{\alpha 1}$ = 1.540598 Å), which suggests a similar in-plane structure and a similar turbostratic disorder for all the compounds. As shown previously for alkyl carboxylate and alkyl sulfate derivatives,[57,58] the structure of the inorganic layer in cobalt hydroxide systems can be described as a triple-deck sheet deriving from the structure of the analogous [$Zn_5(OH)_8(NO_3)_2$]·$2H_2O$.[59,60] It is formed of a monolayer of octahedral Co^{II} hydroxide (Brucite-type structure) with metal vacancies counter-balanced by the occurrence of tetrahedral Co^{II} sites on both sides of the octahedral monolayer.

Considering the thickness of the inorganic layer (7.3 Å[58]), the basal spacing of the functionalized cobalt hydroxide hybrids accounts well for the perpendicular insertion into the inorganic layers of the salen-type complexes, the size of which may be estimated to be about 15 Å from published structures.[50]

For the copper compounds, as shown for the hybrid alkyl carboxylate, alkyl sulfate, or alkyl sulfonate layered copper hydroxides,[57,61–67] the structures of the inorganic layers consist of a quasi-planar triangular array of octahedral copper(II) ions.[68,69]

The basal spacings of the Cu–SED–M compounds (M = Cu, Ni, Co, "MnCl") are in good agreement with the sizes of the SED-H_2–M complexes and the thicknesses of the inorganic layers (about 2.5 Å[68]). The noticeable exception in this series concerns the case of the insertion of the SED-H_2–Zn complex, which leads to a lamellar material with a much larger basal spacing (22.6 Å). Moreover, the XRD pattern of this compound exhibits features at around 33 and 60°, similar to those observed in the cobalt hydroxide derivatives and considered as typical of the formation of a triple inorganic layer. The elemental analysis also shows a net excess of Zn with respect to what is expected for a simple insertion-grafting of SED-H_2–Zn. One hypothesis is that this compound results from the partial decomplexation of the SED-H_2–Zn complex and the subsequent formation of a heterometallic triple inorganic layer containing Cu^{II} in an octahedral environment and Zn^{II} in tetrahedral sites. This phenomenon has already been described for the insertion-grafting of the sulfonated analogue complex.[32]

The interlamellar distances observed after the insertion of the other complexes, SCD-K_2–M M and SBD-H_2–M (M = Co and "MnCl"), are also larger (by about 3 Å) than expected for "simple" insertion-grafting of the complexes. Yet, for these compounds, elemental analysis does not show any excess of the metal cation from the starting complex, and the XRD pattern does not show any peak corresponding to the formation of a triple inorganic layer. Finally, we noticed that thermal treatment of the compounds (heating of the powder samples in an oven at 80 °C for 24 h) led to the irreversible formation of dehydrated compounds with interlamellar distances of around 18.6 Å, in agreement with what was obtained from the grafting of SED-H_2–M M (M = Co, Cu, Ni, "MnCl"; see the example of Cu-SCD–M MnCl in Figure 3). Therefore, we propose that the as-synthesized copper hydroxide compounds are actually hydrated compounds, with water in the interlamellar space and

Table 1. Experimental basal spacing in the hybrid compounds.

Co hydroxide hybrid compound	d_{00l} [Å]	Cu hydroxide hybrid compound	d_{00l} [Å]
Co–SED–Cu	22.4	Cu–SED–Cu	18.6
Co–SED–Ni	22.3	Cu–SED–Ni	18.6
Co–SED–Co	22.3	Cu–SED–Co	18.6
Co–SED–Zn	nonlamellar compound	Cu–SED–Zn	22.6
Co–SED–MnCl	22.3	Cu–SED–MnCl	18.6
Co–SCD–Co	22.4	Cu–SCD–Co	20.8
Co–SCD–MnCl	22.1	Cu–SCD–MnCl	20.9/18.6 after thermal treatment
Co–SBD–Co	22.4	Cu–SBD–Co	21.4
Co–SBD–MnCl	22.6	Cu–SBD–MnCl	21.6
Co–SBD–AlCl	22.3		

strongly involved in hydrogen bonding, which prevents the connection of all of the carboxylate groups of the complexes and increases the interlamellar spacing (Scheme 2).

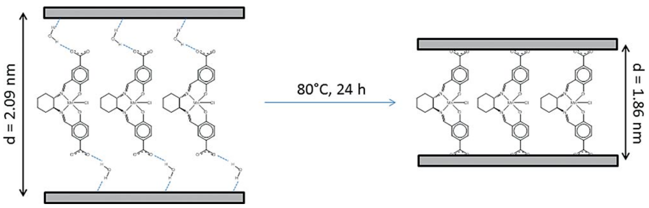

Scheme 2. Evolution of the structures of the Cu–SCD–M and Cu–SBD–M compounds and their influence on the basal spacing upon dehydration.

Yet it appears that in most cases this dehydration process degrades the crystallinity of the materials. Therefore, in the following we will focus on the hydrated samples, which were found to remain stable (and hydrated) for several weeks.

Note that no 00*l* diffraction lines from the starting hydroxides [$Co_2(OH)_3(DS_0)$] and [$Cu_2(OH)_3(DS)$] were evidenced, which indicates the completeness of the reactions. This was further confirmed by FTIR spectroscopy (see below) and elemental analysis (see the Exp. Sect.). The insertion rates, determined from the elemental analyses, are in the same range for all compounds, ranging from 0.2 to 0.35 inserted complexes per Co or Cu ion of the hydroxide host.

FTIR Spectroscopy

The FTIR spectra of the Schiff base complex based hybrids exhibit common features (see the Supporting Information). Typical spectra of the hybrid compounds, the complex, and the hydroxide precursors are presented in Figure 4. The complete list of absorption bands is given in Table SI1 in the Supporting Information. Assignments were made by comparison with the literature.[70–76]

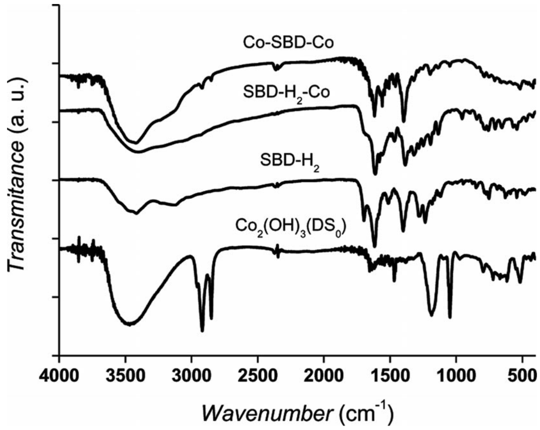

Figure 4. FTIR spectra of the hybrid compound Co–SBD–Co, the parent compounds SBD-H_2 and SBD-H_2–Co, and the cobalt hydroxy dodecyl sulfonate [$Co_2(OH)_3(DS_0)$].

After the exchange reaction, the spectra of all the hybrids indicate the almost complete disappearance of the very strong CH and CH_2 absorption bands at $\tilde{\nu}$ = 2925 and 2854 cm^{-1} and the vanishing of the –SO_3 or –SO_4 bands at $\tilde{\nu}$ = 1300–1000 cm^{-1} arising from the dodecyl sulfate or dodecyl sulfonate in the copper or cobalt hydroxide precursors, respectively.[31,32,77] Concomitantly, characteristic bands of the Schiff base complexes are observed, for which the data are summarized in Table SI1 in the Supporting Information.

A sharp and strong absorption band assigned to the imine C=N group is observed at $\tilde{\nu}$ = 1616 cm^{-1} for the free ligands SBD-H_2, SED-H_2, and SCD-K_2. A set of vibrations assigned to aromatic C=C group is detected in the range $\tilde{\nu}$ = 1580–1430 cm^{-1}.[76] The vibrations of the phenol groups appear in the range 1120–1200 cm^{-1}. The antisymmetrical and symmetrical vibrations of the carboxyl functions are observed at $\tilde{\nu}_{as}$ = 1680–1700 cm^{-1} and $\tilde{\nu}_s$ = 1380–1401 cm^{-1} for the SBD-H_2 and SED-H_2 derivatives. The difference between the two components $\Delta\tilde{\nu}$ is 268–326 cm^{-1}. In the carboxylate salt SCD-K_2, $\tilde{\nu}_{as}$ shifts to 1627–1640 cm^{-1} due to coordination to potassium, and $\Delta\nu$ = 233–264 cm^{-1}. The characteristic bands of the C=C and C–C bonds of the phenyl, ethylene, benzene, or cyclohexanediamine groups are observed in the regions 1450–1580 and 1230–1330 cm^{-1}. The energies of the vibrations are slightly higher for the SBD and SCD than for the SED compounds. The absorptions at 1122–1136 and 1180–1197 cm^{-1} have been assigned to C–O. All compounds, including the starting ligands and their complexes, exhibit strong and very broad IR absorption bands in the regions 3450–3000 cm^{-1} [ν(OH)] and 1030–1089 cm^{-1} [δ(OH)], which have been ascribed to the significant presence of lattice water and hydrogen bonds. After complexation with transition-metal ions, additional bands, slight shifts, or variation of intensities were observed. However, no systematic variation can be identified in these sets of superimposed absorption signals. M–N and M–O bands are observed at high energy in the region 420–665 cm^{-1}.

After grafting the salens onto the hydroxide layers, one notices the systematic shift of the antisymmetrical vibration of the carboxylate functions [ν_{as}(COO)] to higher energy leading to $\Delta\tilde{\nu}$ values similar to those observed for the potassium salts. This observation is consistent with a unidentate coordination of the carboxylate moieties to the metal ions in the hydroxide layers with possible hydrogen bonding to pendant hydroxy groups.[78,79] Moreover, the typical very strong signals of the C–H vibrations ($\tilde{\nu}$ = 2925 and 2854 cm^{-1}) and those stemming from the dodecyl sulfates or dodecyl sulfonates in the copper or cobalt hydroxide precursors ($\tilde{\nu}$ = 1300–1000 cm^{-1}) systematically vanish in the hybrid compounds. Concomitantly, characteristic bands of the Schiff base complexes are observed, which are summarized in Table SI1 in the Supporting Information. These features support the complete anion exchange of the alkyl anions by the Schiff base complexes.

Scanning Electron Microscopy

The hybrid compounds were obtained as thin platelet-shaped microcrystals, in agreement with the lamellar character of their structures. The morphologies and sizes of the microcrystals are very similar to those of the starting materials, in agreement with the powder X-ray diffraction patterns (Figure 5). Furthermore, the composition analysis by EDX (cartography of a 10^4 µm^2 area along with several 1 µm^2 spot analyses) underlines the homogeneity of the different compounds.

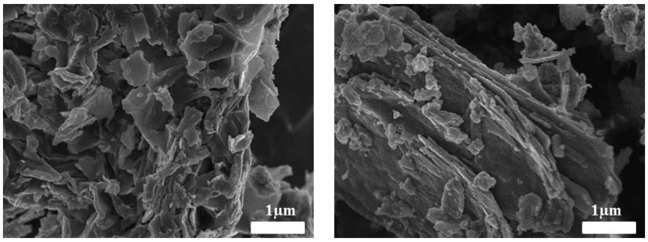

Figure 5. SEM image of Co–(*R*,*R*)-SCD–Co (left) and Cu–(*S*,*S*)-SCD–Co (right).

Thermal Analysis

The thermal stabilities of all the hybrid compounds were investigated in air up to 900 °C. We essentially focus here on the differential thermal and gravimetric analysis (DTA/TGA) of the cobalt hydroxide based systems. The copper hydroxide analogues exhibit a similar behavior. The thermal decomposition of Co–SED–MnCl, Co–SCD–MnCl, and Co–SBD–MnCl is presented in Figures SI4 and SI5 in the Supporting Information as examples. The results indicate that the decomposition occurs in two stages.

The first weight loss is observed between ambient temperature and 160 °C. This first decrease of 11–15% corresponds to the loss of water molecules, in agreement with the chemical formulae of the compounds. This step is extended to temperatures much higher than 100 °C, which indicates that some of the water molecules interact strongly with the inorganic layers. The latter can be involved in a hydrogen-bonding network. This is markedly true in the cases of Co–SCD–M and Cu–SCD–M, for which the release of water is observed up to 160 °C.

The second step is observed between 150 and 300 °C with a weight loss of 38–40%. This loss has been assigned to the degradation of the inserted metal complexes and inorganic layers in an exothermal process, as shown in the TDA plots.

At 900 °C, the final product is a black powder consisting of a mixture of Co_3O_4 or CuO with MnO_2, or other mixed spinel oxides $Co_{3-x}M_xO_4$ (M = Cu, Mn, Ni, Fe, Zn).

As emphasized before, specific thermal variation of the interlayer distances was observed for the Cu–SCD–M and Cu–SBD–M compounds. The TGA/DTA curves of Cu–(*S*,*S*)-SCD–Co are shown as examples in Figure SI6 in the Supporting Information. One notices a weight loss due to the release of water molecules up to 160 °C, which indicates a strong interaction with the inorganic layers. The evolution of the XRD patterns after "annealing" at 80 °C for 24 h indicates that these water molecules can be released by long thermal treatment at a lower temperature.

UV/Vis Spectroscopy

The electronic transitions of the salen ligands, their complexes, and the layered hybrids were identified by UV/Vis spectroscopy. We present in Figures 6, 7, and 8 the spectra recorded for copper and cobalt hydroxides functionalized with some of the complexes. For a given ligand, other metal complexes exhibit similar features.

In the UV region, the intense absorptions of the Schiff base molecules can be attributed to π–π* transitions corresponding to the conjugation of imine with the aromatic rings and to the aromatic rings themselves superimposed upon the n–π* transition of the azomethine.[80] In the case of SBD-H_2, these bands are broadened and shifted towards smaller energies compared with SED-H_2 and SCD-K_2 due to the additional conjugation induced by the aromatic bridge.

The corresponding complexes exhibit d–d transitions in the visible region. For instance, SED-H_2–Ni exhibits a transition at λ = 550 nm assigned to the d–d transition of Ni^{II} ions ($d_{xy}\rightarrow d_{x^2-y^2}$, that is, ${}^1A_1\rightarrow{}^1B_1$ in C_{2v} symmetry).[81] For

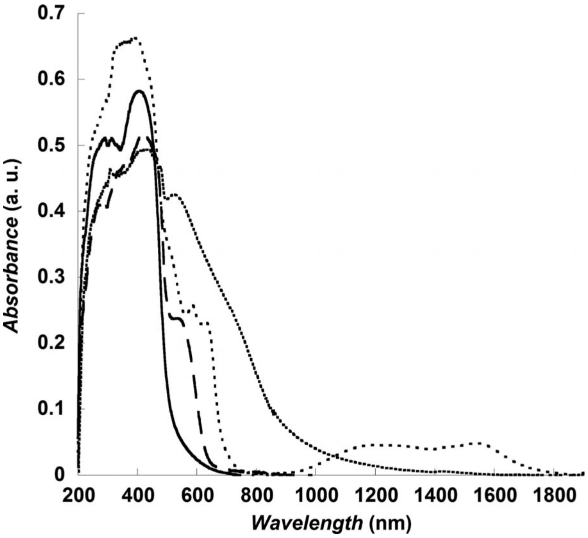

Figure 6. Solid-state UV/Vis absorption spectra of SED-H_2 (full line), SED-H_2–Ni (dashed line), Co-SED–Ni (spaced dotted line), and Cu–SED–Ni (closely dotted line).

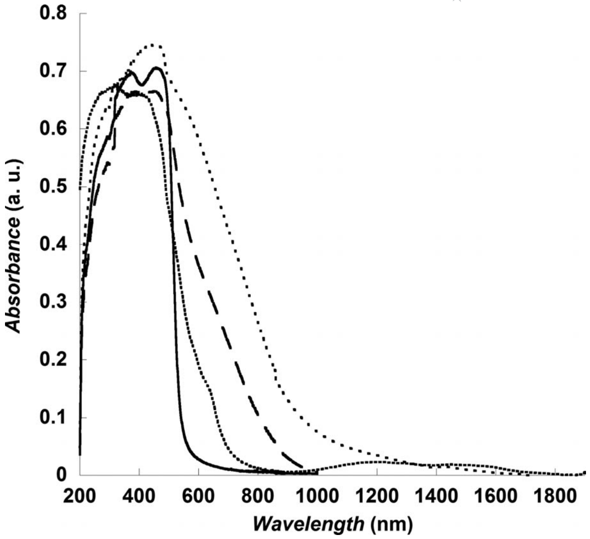

Figure 8. Solid-state UV/Vis absorption spectra of SBD-H_2 (full line), SBD-H_2–AlCl (dashed line), Co–SBD–AlCl (spaced dotted line), and Cu–SCD–AlCl (closely dotted line).

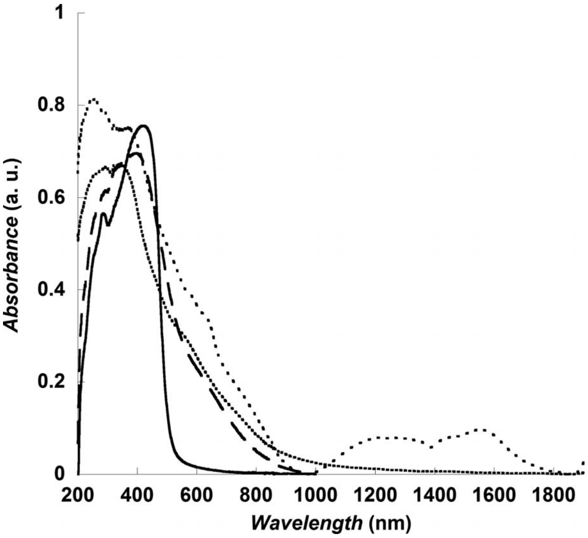

Figure 7. Solid-state UV/Vis absorption spectra of SCD-K_2 (full line), SCD-K_2–MnCl (dashed line), Co–SCD–MnCl (spaced dotted line), and Cu–SCD–MnCl (closely dotted line).

the cobalt and manganese complexes, large bands at around 600 nm appear and can be assigned to the d–d transition of the complexed metal [$^4T_{1g}(F) \rightarrow {}^4T_{1g}(P)$ for the Co^{II} complexes, and $^5E_g \rightarrow {}^5T_{2g}$ for the Mn^{III} complexes].[80]

Finally, in the copper and cobalt hybrid hydroxides, the electronic transitions of the complexes overlay the transitions arising from the inorganic structures. In the UV region, the charge transfer O→M (M = Co or Cu) of the inorganic layers is superimposed upon the ligand transitions. For the cobalt hybrids (particularly visible in the spectrum of Co–SED–Ni), four additional bands are observed in the Vis/NIR region. Two of the bands, at around 580 and 1200 nm, have been attributed to high-spin (HS) d^7 Co^{II} ions in octahedral sites [$^4T_{1g}(F) \rightarrow {}^4T_{1g}(P)$ and $^4T_{1g}(F) \rightarrow {}^4T_{2g}(F)$ transitions, respectively], whereas the other two, at around 640 and 1550 nm, can be attributed to d^7 Co^{II} ions in tetrahedral sites [$^4A_2(F) \rightarrow {}^4T_1(P)$ and $^4A_2(F) \rightarrow {}^4T_1(F)$ transitions, respectively].[82] These features are in accordance with the proposed structures and with the magnetic behavior (see below).[59,83] The d–d transition of the Ni^{II} ion appears as a shoulder at 520 nm. In the case of the insertion of Mn or Co complexes, absorption due to the cobalt ions of the inorganic layers hides the d–d transitions of the metals of the inserted complexes.

In the copper hydroxide series, the broad absorption band centered at $\lambda \approx 560$ nm, typical of the Cu^{II} ion in the octahedral geometry ($^2E_g \rightarrow {}^2T_{2g}$), also masks the transitions of the metals of the inserted complexes.

Optical Circular Dichroism

The two SCD-based series [(*R*,*R*) and (*S*,*S*)] give identical UV spectra. The optical circular dichroism (OCD) spectra of the hybrid compounds show that the insertion of a chiral complex leads to chiral hybrid compounds (Figure 9). The chirality is evidenced by the symmetry of the OCD spectra of Cu–(*R*,*R*)-SCD–MnCl and Cu–(*S*,*S*)-SCD–MnCl [and of Co–(*R*,*R*)-SCD–MnCl and Co–(*S*,*S*)-SCD–MnCl]. Three regions can be distinguished in the spectra. Below 300 nm, the dichroic signal of the hybrid compounds is almost zero, whereas it is quite strong in the complex alone (see Figure SI7 in the Supporting Information) because of the strong O→M charge transfer (M = Co or Cu) of the inorganic layers in this region. The signals between 300 and 500 nm correspond to the dichroic signals of the π–π*, n–π*, and d–π* transitions of the inserted complex. In the third region, above 500 nm, the sign of the signal depends on the hydroxide host (Co or Cu), whereas the sign of the signal in the high-energy region remains the same irrespective of the metal cation of the inorganic host. Moreover, the OCD spectra of the hybrids in this region exhibit signs and shapes different to those of the complexes alone. Therefore, this low-energy signal cannot be assigned only to the $^5E_g \rightarrow ^5T_{2g}$ transition of the Mn^{III} complex, but may result from a combination of signals arising from the inserted complex and the d–d transitions of the cations within the hydroxide layers. This combination was not observed in the case of the insertion of chiral salensulfonate complexes.[31] Such an interaction suggests that the carboxylate groups are more efficient than sulfonates for a real chirality transfer from the salen to the inorganic layers.

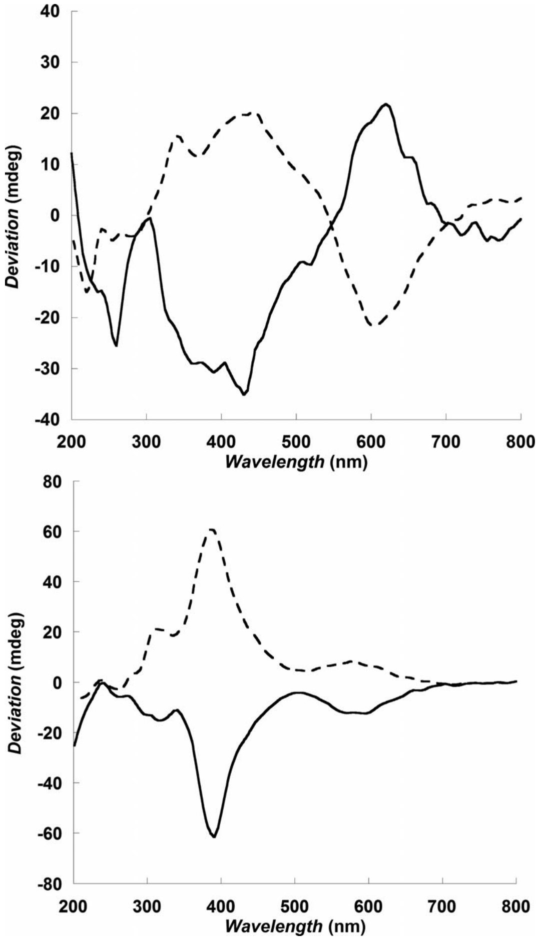

Figure 9. Solid-state OCD spectra of Co–(*R*,*R*)-SCD–MnCl (full line) and Co–(*S*,*S*)-SCD–MnCl (dashed line) (above) and Cu–(*R*,*R*)-SCD–MnCl (full line) and Cu–(*S*,*S*)-SCD–MnCl (dashed line) (below).

Magnetic Properties

All copper hydroxide based hybrid compounds except for Cu–SED–Co and Cu–SBD–Co show an overall antiferromagnetic behavior without ordering down to 1.8 K irrespective of the nature of the complex inserted (see the Supporting Information). For Cu–SED–Co and Cu–SBD–Co, the χT versus T curves suggest a weak ferrimagnetic ordering at very low temperature (ferromagnetic or canted antiferromagnetic). This behavior was confirmed by the magnetization versus field measurements at 1.8 K. A rather sharp increase in the magnetization was observed at low fields, and the magnetization value at high field was almost saturated, but low and far from the expected value for full alignment of the moments borne by the copper ions and the inserted complexes. The low-temperature ac susceptibility measurements showed only the basis of growing peaks in the χ'' (out-of-phase susceptibility) signals, which indicates that long-range order is not fully established at 1.8 K.

All of the cobalt hydroxide based hybrid compounds exhibit similar behavior. Selected characteristic data are collected in Table 2. The Curie constants are in agreement with the proposed formulae (see the Exp. Sect.), considering a contribution of 2.2–2.8 emu K mol^{-1} for the Co^{II} ions in tetrahedral sites, 2.8–3.4 emu K mol^{-1} for the Co^{II} ions in octahedral sites,[84] and the usual values for the transition metal of the complexes inserted in between the inorganic layers.

Table 2. Magnetic characteristics of the cobalt hybrid compounds.

Compound	C [emu K mol^{-1}]	T_N [K]	$\mu_0 H_C$ [T]	M_{5T} [μ_B]
$Co_2(OH)_3DS_0$	5.04	6.7	0.14	2.08
Co–SED–Cu	5.23	12.8	0.30	2.24
Co–SED–Ni	4.99	10.4	0.25	2.10
Co–SED–Co	5.69	7.5	0.09	2.98
Co–SED–MnCl	8.14	6.8	0.08	3.87
Co–(*R*,*R*)-SCD–Co	5.70	7.2	0.09	3.30
Co–(*R*,*R*)-SCD–MnCl	6.12	6.5	0.07	3.26
Co–SBD–MnCl	8.55	9.6	0.07	3.60
Co–SBD–Co	7.06	6.8	0.07	3.79
Co–SBD–AlCl	5.56	6.8	0.06	3.47

As an example, we report in Figures 10, 11, and 12 the results concerning Co–SED–Cu. As the temperature decreases from room temperature, the χT product slightly decreases to a minimum at around 90 K. This small decrease is well understood on the basis of a single-ion spin–orbit coupling effect and/or antiferromagnetic interactions between the Co^{II} moments. Below this minimum, the χT prod-

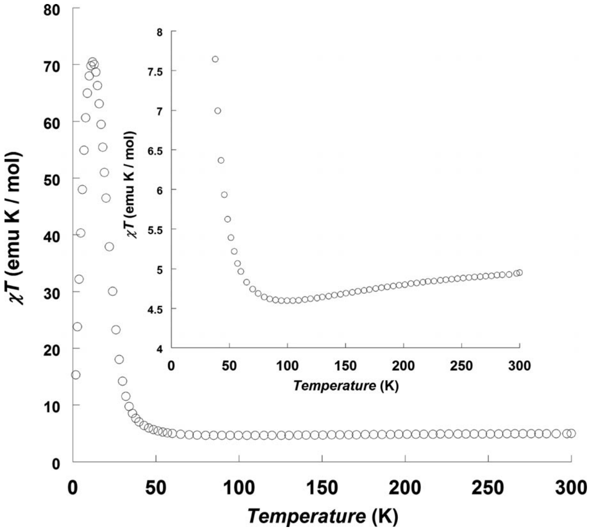

Figure 10. χT vs. T curve for Co–SED–Cu (under 500 Oe applied dc field).

uct exhibits a steep increase to a maximum at 11.3 K (71 emu K mol^{-1}). This increase can be related to the occurrence of long-range ferromagnetic order (Figure 10).

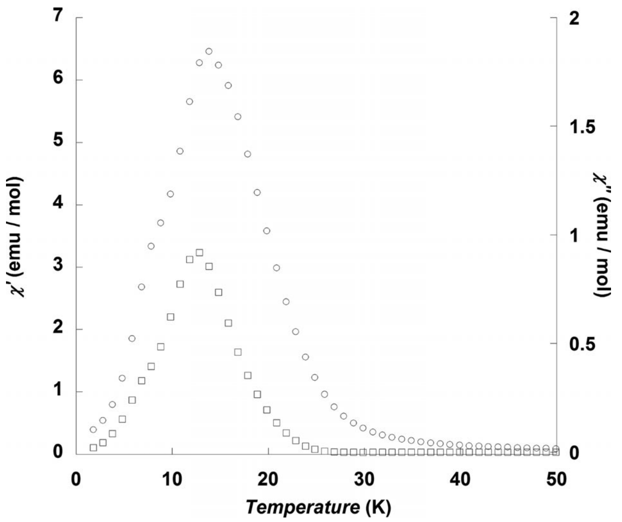

Figure 11. ac susceptibility measurements for Co–SED–Cu (0.35 mT, 100 Hz; open circles: in-phase susceptibility; open squares: out-of-phase susceptibility).

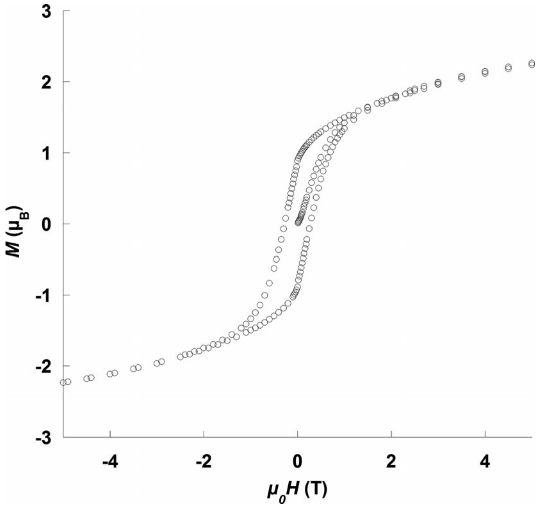

Figure 12. *M* vs. *H* curve for Co–SED–Cu at 1.8 K.

The ordering temperatures were determined by ac susceptibility measurements (f = 100 Hz, μ_0H_{ac} = 0.35 mT, Figure 11). The maximum of the real part, χ', leads to a T_N value of 12.8 K for Co–SED–Cu.

The ferromagnetic-type behavior is confirmed by the magnetization versus field curve at low temperature (Figure 12), which shows the presence of a hysteresis loop with a coercive field of 0.3 T at 1.8 K. The low value of the moments at high field compared with that expected for a total alignment of the moments (4–6 μ_B for two Co^{II} plus the expected value for the inserted metal ion) confirms the ferrimagnetic ordering.

Despite the fact that there is no clear general tendency in the evolution of the magnetic properties of the hybrids depending on the inserted complex, it is worth noting that there are indeed important differences in the ordering temperatures for a given organic ligand when the inserted metal ion is changed. This indicates that the inserted cations participate, at least partly, in the establishment of the magnetic ordering, which suggests the occurrence of a noticeable magnetic exchange interaction between the inorganic layers and the inserted complexes. Note that the analogue hybrids involving disulfonate complexes showed almost no influence of the inserted cation on the magnetic ordering temperatures.[31,32] Thus, it appears that carboxylate anchoring functions are more efficient than sulfonate groups in promoting magnetic interactions and hence in controlling the magnetic behavior of the hybrid systems.

Conclusions

In our previous work on the functionalization of layered single metal hydroxides (LSHs) with metal complexes we were able to insert some salendisulfonate complexes. Initially, the sulfonate anchoring groups were chosen to facilitate the dissolution of the complexes in water. Yet our results highlighted some limitations. First, the disulfonate Schiff base complexes were found to be sensitive to hydrolysis during the anion-exchange reactions carried out in aqueous media. To limit hydrolysis, we developed a new approach involving the pre-insertion of long alkyl chain sulfonates or sulfates. As a result, the interlamellar space was greater and more hydrophobic. Secondly, concomitant cation exchange with the metal of the hydroxide layers was observed in some cases, inducing a significant change in the structure of the inorganic host. To overcome this, we decided to functionalize the LSH with dicarboxylate complexes, which were expected to be more stable. Moreover, it was particularly interesting to investigate the influence of the anchoring groups (carboxylates versus sulfonates) on the properties of the hybrid systems.

In this work we synthesized numerous transition-metal Schiff base dicarboxylate complexes, including complexes of trivalent metals. These complexes were successfully inserted and grafted into copper and cobalt LSHs. No hydrolysis occurred, and we observed no double exchange except with the Cu–SED–Zn system. In fact, the zinc complex is the more labile one. Hence, the carboxylate moieties really improve the robustness of the salen complexes in comparison with the sulfonates. Another difference of the sulfonate analogues concerns the interaction of the complexes with the inorganic host. We noticed that the magnetic ordering temperature of the cobalt hydroxide hybrids varies with the metal in the series of complexes studied in this work. This was not the case for the sulfonate analogues, which indicates a better coupling with the carboxylates than with the sulfonates. The sulfonate group is usually known as a ligand that hampers efficient magnetic coupling.[85,86] This difference is merely a result of the higher spin density along the C–C bond of the carboxylates than along the C–S bond of the sulfonates within the anchoring moieties.[86–88] Thus, functionalization through carboxylate bridges is more efficient for the tuning of the magnetic properties of these layered hybrid systems, all the more so as we can vary the metal ion in the salen complexes.

More generally, immobilization and grafting into the layered hydroxides of such a variety of metal complexes with different functionalities gives, in principle, many possibilities for adapting these hybrid materials to different applications. Some possibilities were investigated. Concerning the transfer of chirality, the carboxylate group again seems more efficient than the sulfonate. As a possible application, we tested the enantiocatalytic activity of M–[(*R*,*R*)- or (*S*,*S*)]-SCD–MnCl (M = Cu or Co) in the epoxidation of styrene. The hybrid system was stable under the alkaline and oxidative conditions of the reaction. Nevertheless, we observed no significant activity, contrary to what was reported by Bhattacharjee et al. for Zn-Al layered double hydroxide based systems.[20] This difference could arise from the different specific area and accessibility of the salen complex embedded within the hydroxide host. Recently, we have shown in peptide inserted hydroxides that molecules inserted in LSH are accessible to small ions.[16] We envision testing the chiral compounds of this study for catalytic activity towards molecules in the gas phase.

We also investigated the optical properties of the hydroxides encompassing Al^{3+} salen complexes, which have been reported to show intense blue luminescence with adjustable quantum yields.[48] In the hybrid structures, the luminescence was apparently quenched as a result of absorption by the inorganic layers. Such quenching was also observed in LSHs containing oligothiophenedicarboxylates[89] whereas photoluminescence was maintained in oligo(phenylene–vinylene) (OPV) systems.[29] Our results indicate that the emission wavelengths of the molecular dyes and their distance to the inorganic layers has to be adjusted in order to obtain luminescent hybrids. This could be achieved by appropriate modification of the complexes. For instance, longer carboxylate anchoring arms can be grafted onto the salen core. Several other applications can be explored for these new hybrid multifunctional systems depending on the metal ions involved in the complex. As a result of the current improvements in the control of the anion-exchange reaction we have shown that the insertion and grafting of metal complexes into layered single metal hydroxides is a tractable and appealing approach towards new functional materials.

Experimental Section

Methods: Elemental analyses for C, H, N, S, and metals were carried out by the Service de Microanalyses of the University of Strasbourg and by the Service Central d'Analyse of the CNRS (USR-59). The powder XRD patterns were collected with a Bruker D8 ADVANCE diffractometer (Cu-$K_{\alpha 1}$, $\lambda = 1.540598$ Å) equipped with the energy discriminating detector SolX. ^{1}H NMR spectra were recorded with a Bruker AVANCE 300 (300 MHz) spectrometer. The peaks of nondeuteriated solvents were used as internal references. The SEM images were obtained with a JEOL 6700F scanning electron microscope equipped with a field emission gun operating at 3 kV in the SEI mode. FTIR spectra were collected with a Digilab FTS 3000 computer-driven instrument (0.1 mm thick powder samples ca. 1% in KBr) in transmittance with a resolution of 4 cm^{-1} [software: Digilab Merlin 3.4; laser He-Ne; detector MCT (Cryogenic Mercury CadmiumTellurid); source: standard ceramic]. UV/Vis/NIR studies were performed with a Perkin–Elmer Lambda 950 spectrometer (spectra recorded in reflection mode using a 150 mm integrating sphere with a mean resolution of 2 nm and a sampling rate of 300 nm min^{-1}). Optical circular dichroism spectra were recorded as powders diluted in KBr pellets (ca. 1% weight) with a Jasco 810 spectrometer. The data were corrected for the background signal of a pellet of pure KBr of the same dimensions. TGA/TDA experiments were performed by using a Texas Instruments SDT Q600 instrument (heating rates of 5 °C min^{-1}, air stream, platinum crucible). Magnetic studies were performed with a SQUID magnetometer (Quantum Design MPMS-XL) in the temperature and field ranges of 2–300 K and ±5 T, respectively; ac susceptibility measurements were performed in a 0.35 mT alternative field (100 Hz). Magnetization measurements at different fields at room temperature confirmed the absence of ferromagnetic impurities.

Synthesis of [$Cu_2(OH)_3(C_{12}H_{25}SO_4)$]·$0.5H_2O$ and [$Co_2(OH)_3$-($C_{12}H_{25}SO_3$)]: [$Co_2(OH)_3(DS_0)$] and [$Cu_2(OH)_3(DS)$] were synthesized according to protocols published in previous works.[58,63] All experiments were conducted under argon, and the solvents were degassed prior to use. The yields of the hybrid compounds were around 50–70%.

Ligand Synthesis

3-Formyl-4-hydroxybenzoic Acid (FBA-H): 3-Formyl-4-hydroxybenzoic acid was synthesized according to a published procedure.[48] In a 500 mL flask, *p*-hydroxybenzoic acid (15 g, 108 mmol) was added to trifluoroacetic acid (40 mL) to form a suspension. A solution of hexamethylenetetraamine (15.3 g, 109 mmol) in trifluoroacetic acid was added dropwise under Ar. After heating at reflux under Ar for 2 h, the reaction mixture turned a transparent yellow. After cooling to ambient temperature, the solution was stirred with 4 M HCl (300 mL) for 3 h. The yellowish solid was filtered, washed with water (10× 100 mL), and dried under vacuum. Yield: 40%. ^{1}H NMR (300 MHz, [D$_6$]DMSO): δ = 7.06 (d, J = 8.82 Hz, 1 H), 8.0 (dd, J_1 = 2.43, J_2 = 8.82 Hz, 1 H), 8.21 (d, J = 2.22 Hz, 1 H), 10.28 (s, 1 H) ppm. $C_8H_6O_4$·$0.2H_2O$ (169.73): calcd. C 56.75, H 3.76; found C 56.72, H 3.88.

Salendicarboxylic Acid (SED-H$_2$): FBA-H (1.08 g, 6.5 mmol) was dissolved in ethanol (30 mL), and a solution of ethylenediamine (217 μL, 3.25 mmol) in ethanol (30 mL) was added dropwise. The reaction led to a yellow-orange precipitate. The mixture was heated at reflux for 1 h and then cooled to room temperature. SED-H$_2$ was isolated by filtration, washed with ethanol, and dried under vacuum. Yield: 50%. ^{1}H NMR (300 MHz, [D$_6$]DMSO): δ = 3.94 (s, 4 H), 6.83–6.87 (d, J = 8.82 Hz, 2 H), 7.82–7.86 (dd, J_1 = 2.22, J_2 = 8.61 Hz, 2H$_b$), 8.03–8.05 (d, J = 2.01 Hz, 2 H), 8.71 (s, 2 H) ppm. $C_{18}H_{16}N_2O_6$·$0.8H_2O$ (371.3): calcd. C 58.22, H 4.76, N 7.54; found C 58.22, H 4.87, N 8.12.

Dipotassium (*R*,*R*)-Cysalendicarboxylate [(*R*,*R*)-SCD-K$_2$]: Dipotassium (*R*,*R*)-cyclohexanediamine monotartrate (2.64 g, 10 mmol) was dissolved in water/MeOH (60 mL, 1:1, v/v) along with K_2CO_3 (2.76 g, 20 mmol). An ethanolic solution (60 mL) of FBA-H (3.32 g, 20 mmol) was added dropwise leading to a precipitate. After complete addition, the reaction mixture was heated at reflux for 1 h and filtered immediately. The filtrate was concentrated to yield a solid, which was recrystallized from ethanol. Yield: 91%. $[\alpha]^{20}_{D}$ = +150 deg dm^{-1} cm^3 g^{-1} (c = 0.001 mol L^{-1}, methanol). ^{1}H NMR

(300 MHz, [D$_6$]DMSO): δ = 1.45–9 (m, 8 H), 3.49 (s, 2 H), 7.69–7.74 (dd, J_1 = 1.98, J_2 = 8.37 Hz, 2 H), 7.79–7.8 (d, J = 1.77 Hz, 2 H), 8.48 (s, 2 H) ppm. $C_{22}H_{20}K_2N_2O_6\cdot 2.8H_2O$ (535.72): calcd. C 49.32, H 4.76, N 5.23; found C 49.29, H 4.35, N 5.18.

Dipotassium (*S*,*S*)-Cysalendicarboxylate [(*S*,*S*)-SCD-K$_2$]: The same procedure as above was used, starting from dipotassium (*S*,*S*)-cyclohexanediamine monotartrate. $[\alpha]_D^{20}$ = –174 deg dm^{-1} cm^3 g^{-1} (c = 0.001 mol L^{-1}, methanol).

Phenylenesalendicarboxylic Acid (SBD-H$_2$): *o*-Phenylenediamine (0.36 g, 3.3 mmol) was dissolved in methanol (30 mL). A methanolic solution (40 mL) of FBA-H (1.1 g, 6.6 mmol) was added leading to the formation of a precipitate. After stirring at ambient temperature for 2 h, the volume of the mixture was reduced to 1/3 by concentration under reduced pressure. The solid was collected by filtration, washed with ethanol and diethyl ether, and dried under vacuum. Yield: 57%. ^{1}H NMR (300 MHz, [D$_6$]DMSO): δ = 7.01–7.05 (d, J = 8.82 Hz, 2 H), 7.41–7.45 (m, 2 H), 7.50–7.54 (m, 2 H), 7.93–7.97 (m, 2 H), 8.33–8.35 (m, 2 H), 9.06 (s, 2 H) ppm. $C_{22}H_{16}N_2O_6\cdot 0.8H_2O$ (418.98): calcd. C 63.06, H 4.76, N 6.68; found C 62.99, H 4.42, N 7.34.

Synthesis of Complexes with SED-H$_2$

SED-H$_2$–Co: SED-H$_2$ (0.17 g, 0.46 mmol) was partially dissolved in DMF (40 mL) under argon. Then a solution of $Co(OAc)_2\cdot 4H_2O$ (84 mg, 0.42 mmol) in DMF (40 mL) was added dropwise under argon. The solution turned a clear blue. A brown solid precipitated upon addition of methanol (100 mL), which was collected by filtration, washed with methanol, and dried under vacuum. Yield: 65%. $C_{18}H_{14}N_2O_6Co\cdot 2.7DMF$ (610.35): calcd. C 51.36, H 5.43, N 10.78; found C 51.19, H 5.27, N 10.72.

SED-H$_2$–Cu: The green solid was synthesized similarly to above starting from $Cu(OAc)_2\cdot H_2O$. Yield: 50%. $C_{18}H_{14}CuN_2O_6\cdot 1.5H_2O$ (444.91): calcd. C 48.59, H 3.82, N 6.29; found C 48.60, H 3.74, N 7.01.

SED-H$_2$–Zn: The yellow solid was synthesized similarly to above starting from $Zn(OAc)_2\cdot H_2O$. Yield: 45%. $C_{18}H_{14}N_2O_6Zn\cdot 1.8DMF$ (565.28): calcd. C 49.72, H 4.74, N 9.42; found C 49.98, H 4.51, N 9.87.

SED-H$_2$–Ni: SED-H$_2$ (0.18 g, 0.48 mmol) was dissolved in a mixture of water (30 mL) with a few drops of NaOH. An aqueous solution (20 mL) of $Ni(OAc)_2\cdot 4H_2O$ (0.14 g, 0.54 mmol) was then added dropwise under vigorous stirring. After stirring at room temperature for 30 min, an orange precipitate was filtered, washed with water, and dried under vacuum. Yield: 45%. $C_{18}H_{14}N_2NiO_6\cdot 1.9H_2O$ (446.67): calcd. C 48.40, H 3.98, N 6.27; found C 48.41, H 4.34, N 7.09.

SED-H$_2$–MnCl: $Mn(OAc)_2\cdot 4H_2O$ (0.15 g, 0.62 mmol) dissolved in methanol (10 mL) was added to a suspension of SED-H$_2$ (0.22 g, 0.62 mmol) in methanol (50 mL). The color changed from yellow to greenish. After 4 h under reflux, the mixture was cooled to ambient temperature, and a saturated aqueous solution of LiCl (3 mL) was added. A brownish-green solid was filtered, washed with water and methanol, and dried under vacuum. Yield: 64%. $C_{18}H_{14}N_2O_6MnCl\cdot 0.5H_2O$ (454.10): calcd. C 47.6, H 3.32, N 6.17; found C 47.58, H 3.95, N 6.44.

SED-H$_2$–FeCl: Anhydrous $FeCl_3$ (0.27 g, 1.68 mmol) dissolved in ethanol (35 mL) was added dropwise to a suspension of SED-H$_2$ (0.62 g, 1.68 mmol) in ethanol (80 mL) in the presence of triethylamine (467 µL) under an inert gas. The color of the solution changed from yellow to purple-red. After heating at reflux for 2 h, the solution was cooled to ambient temperature, and its volume was reduced to 1/2 by concentration under reduced pressure. The complex was then precipitated with diethyl ether, filtered, washed with diethyl ether, and dried under vacuum. Yield: 84%. $C_{18}H_{14}ClFeN_2O_6\cdot 0.5H_2O$ (454.48): calcd. C 47.57, H 3.33, N 6.16; found C 47.55, H 4.16, N 6.83.

Synthesis of Complexes with SCD-K$_2$

The procedures were the same for both the (*R*,*R*) and (*S*,*S*) enantiomers.

SCD-K$_2$–MnCl: $Mn(OAc)_2\cdot 4H_2O$ (0.77 g, 3.12 mmol) dissolved in water (20 mL) was added rapidly drop-by-drop to a freshly prepared solution of SCD-K$_2$ (1.67 g, 3.12 mmol) in methanol (20 mL). A greenish precipitate formed immediately. Then a saturated aqueous solution of LiCl (3 mL) was added. The mixture was then stirred at room temperature for 2 h, then left to stand for 2 h. The solid was filtered, washed with water and ethanol, and dried under vacuum. Yield: 41%. $C_{22}H_{18}N_2O_6MnCl\cdot 8H_2O$ (636.6): calcd. C 41.63, H 5.69, N: 4.62; found C 41.51, H 5.38, N 4.36.

SCD-K$_2$–Co: $Co(OAc)_2\cdot 4H_2O$ (0.26 g, 1.03 mmol) dissolved in water (20 mL) was added rapidly drop-by-drop to a methanolic solution (40 mL) of SCD-K$_2$ (0.55 g, 1.03 mmol). A brown precipitate formed immediately, and the mixture was stirred at room temperature for 2 h. The solid was filtered, washed with methanol, and dried under vacuum. Yield: 90%. $C_{22}H_{18}CoN_2O_6\cdot 6.4H_2O$ (579.87): calcd. C 45.56, H 5.34, N 4.36; found C 45.63, H 5.16, N 4.88.

Synthesis of Complexes with SBD-H$_2$

SBD-H$_2$–MnCl: $Mn(OAc)_2\cdot 4H_2O$ (0.44 g, 1.80 mmol) dissolved in water (10 mL) was added dropwise to a methanolic suspension (20 mL) of SBD-H$_2$ (0.75 g, 1.80 mmol) with a few drops of NaOH. Then a saturated aqueous solution of LiCl (3 mL) was added. The mixture was then stirred at room temperature for 2 h and then left to stand for 2 h. The solid was filtered, washed with water and ethanol, and dried under vacuum. Yield: 45%. $C_{22}H_{14}ClMnN_2O_6\cdot 4.5H_2O$ (573.60): calcd. C 46.06, H 4.00, N 4.88; found C 46.09, H 4.30, N 5.20.

SBD-H$_2$–AlCl: $Al(Et)_2Cl$ (670 µL; 1.30 mmol) was added under argon to an ethanolic suspension (30 mL) of SBD-H$_2$ (0.41 g, 0.99 mmol). The solution became translucent after 2 h of stirring at room temperature under argon. The volume of the mixture was reduced to 1/4 by concentration under reduced pressure. The complex precipitated upon the addition of diethyl ether, collected by filtration, washed with diethyl ether, and dried under vacuum. Yield: 95%. $C_{22}H_{14}AlClN_2O_6\cdot 5.4H_2O$ (561.87): calcd. C 46.03, H 4.41, N 4.98; found C 47.01, H 4.47, N 5.06.

SBD-H$_2$–Co: $Co(OAc)_2\cdot 4H_2O$ (105 mg, 0.42 mmol) dissolved in DMF (40 mL) was added dropwise to a solution of SBD-H$_2$ (0.176 g, 0.42 mmol) in DMF (40 mL). After 2 h of stirring at room temperature, methanol (100 mL) was added, and the precipitate was collected by filtration, washed with methanol, and dried under vacuum. Yield: 77%. $C_{22}H_{14}CoN_2O_6\cdot 0.9DMF\cdot 4.3H_2O$ (604.89): calcd. C 49.04, H 4.07, N 6.71; found C 49.11, H 3.64, N 6.74.

Synthesis of the Hybrid Materials M–SED–M′ (M = Cu, Co; M′ = Co, Cu, Zn, Ni, “MnCl”).

Co–SED–Cu: SED-H$_2$–Cu (0.21 g, 0.47 mmol) was suspended in water (35 mL) and solubilized upon adjustment of the pH to 8 by addition of 0.2 M NaOH. Then $[Co_2(OH)_3(DS_0)]$ (0.20 g, 0.48 mmol) was dispersed into the solution under an inert gas, and ethanol (35 mL) was added. The mixture was then stirred under argon at 80 °C for 5 h. After cooling to room temperature, a light-blue powder was isolated by filtration, washed with water and ethanol, and dried under vacuum. Yield: 92%. $Co_2(OH)_{3.2}$-

$(C_{18}H_{12}N_2O_6Cu)_{0.4}$·$2.8H_2O$ (392.70): calcd. C 22.02, H 3.56, N 2.85, Cu 6.47, Co 30.04; found C 22.10, H 3.48, N 2.89, Cu 6.21, Co 30.20.

Co–SED–Ni: The title compound was obtained according to a procedure similar to that used for Co–SED–Cu. Yield: 80%. $Co_2(OH)_{3.2}$-$(C_{18}H_{12}N_2O_6Ni)_{0.4}$·$2.9H_2O$ (389.12): calcd. C 22.22, H 3.55, N 2.87, Ni 6.01, Co 30.32; found C 22.31, H 3.57, N 2.87, Ni 5.46, Co 30.59.

Co–SED–Co: The title compound was obtained according to a procedure similar to that used for Co–SED–Cu. Yield: 80%. $Co_2(OH)_{2.6}$-$(C_{18}H_{12}N_2O_6Co)_{0.7}$·$6.4H_2O$ (565.23): calcd. C 26.77, H 4.24, N 3.49, Co 28.15; found C 26.83, H 3.85, N 3.43, Co 28.23.

Co–SED–MnCl: The title compound was obtained according to a procedure similar to that used for Co–SED–Cu. Yield: 71%. $Co_2(OH)_{2.44}(C_{18}H_{12}N_2O_6MnCl)_{0.78}$·$7H_2O$ (630.71): calcd. C 26.73, H 4.12, N 3.46, Mn 6.79, Co 18.69; found C 27.47, H 3.97, N 3.38, Mn 6.46, Co 18.35.

Cu–SED–Cu: SED-H_2–Cu (0.21 g, 0.47 mmol) was suspended in water (35 mL) and solubilized upon adjustment of the pH to 8 by addition of 0.2 M NaOH. Then $[Cu_2(OH)_3(DS)]$ (0.22 g, 0.48 mmol) was dispersed into the solution under an inert gas, and ethanol (35 mL) was added. The mixture was stirred under argon at 80 °C for 2 h. A light-blue powder was isolated by filtration, washed with water and ethanol, and dried under vacuum. Yield: 76%. $Cu_2(OH)_3$-$(C_{18}H_{12}N_2O_6Cu)_{0.5}$·$3.2H_2O$ (465.48): calcd. C 25.08, H 3.39, N 3.24, Cu 34.13; found C 25.14, H 3.40, N 2.94, Cu 34.13.

Cu–SED–Ni: The title compound was obtained according to a procedure similar to that used for Cu–SED–Cu. Yield: 76%. $Cu_2(OH)_{3.24}$-$(C_{18}H_{12}N_2O_6Ni)_{0.38}$·$1.1H_2O$ (365.46): calcd. C 22.72, H 2.82, N 2.94, Ni 6.10, Cu 35.63; found C 22.83, H 2.99, N 2.86, Ni 5.42, Cu 35.63.

Cu–SED–Co: The title compound was obtained according to a procedure similar to that used for Cu–SED–Cu. Yield: 66%. $Cu_2(OH)_{2.24}$-$(C_{18}H_{12}N_2O_6Co)_{0.88}$·$4.7H_2O$ (611.43): calcd. C 31.10, H 3.63, N 4.03, Co 8.49, Cu 20.78; found C 31.09, H 3.90, N 4.10, Co 8.12, Cu 20.78.

Cu–SED–MnCl: The title compound was obtained according to a procedure similar to that used for Cu–SED–Cu. Yield: 66%. $Cu_2(OH)_{2.72}(C_{18}H_{12}N_2O_6MnCl)_{0.64}$·$3H_2O$ (510.59): calcd. C 27.10, H 3.24, N 3.51, Mn 6.88, Cu 24.87; found C 27.93, H 3.58, N 4.02, Mn 6.19, Cu 25.12.

Cu–SED–Zn: The title compound was obtained according to a procedure similar to that used for Cu–SED–Cu. Yield: 66%. $Cu_{1.32}$-$Zn_{0.68}(OH)_{2.72}(C_{18}H_{12}N_2O_6Zn)_{0.64}$·$3.4H_2O$ (501.63): calcd. C 27.58, H 3.42, N 3.57, Zn 17.21, Cu 16.72; found C 27.52, H 3.32, N 4.12, Zn 17.19, Cu 16.73.

Synthesis of the Hybrid Materials M–SCD–M′ (M = Co, Cu; M′ = Mn, Co)

Co–(*R*,*R*)-SCD–MnCl: The complex (*R*,*R*)-SCD-K_2–MnCl (0.32 g, 0.5 mmol) was suspended in water (35 mL). The pH of the solution was adjusted to 8 by using 0.2 M NaOH. Then $[Co_2(OH)_3(DS_0)]$ (0.20 g, 0.48 mmol) was dispersed into the solution under an inert gas, and ethanol (35 mL) was added. The mixture was then stirred under argon at 80 °C for 5 h. After cooling to room temperature, a brown powder was isolated by filtration, washed with water and ethanol, and dried under vacuum. Yield: 60%. $Co_2(OH)_{3.26}$-$(C_{22}H_{18}N_2O_6MnCl)_{0.37}$·$3.5H_2O$ (420.16): calcd. C 23.27, H 4.06, N 2.47, Co 28.05, Mn 4.84; found C 23.83, H 4.36, N 1.98, Co 28.19, Mn 4.59.

Co–(*S*,*S*)-SCD–MnCl: The procedure was identical to that above, starting from (*S*,*S*)-SCD-K_2–MnCl. Yield: 60%. $Co_2(OH)_{3.40}$-$(C_{22}H_{18}N_2O_6MnCl)_{0.30}$·$6H_2O$ (432.81): calcd. C 18.32, H 4.84, N 1.94, Co 27.23, Mn 3.81; found C 18.77, H 4.03, N 1.93, Co 27.31, Mn 3.85.

Co–(*R*,*R*)-SCD–Co: The procedure was identical to that above, starting from (*R*,*R*)-SCD-K_2–Co. Yield: 50%. $Co_2(OH)_{3.12}$-$(C_{22}H_{18}N_2O_6Co)_{0.44}$·$4.5H_2O$ (456.73): calcd. C 25.46, H 4.42, N 2.70, Co 31.48; found C 25.74, H 4.17, N 2.50, Co 30.97.

Co–(*S*,*S*)-SCD–Co: The procedure was identical to that above, starting from (*S*,*S*)-SCD–K_2–Co. Yield: 50%. $Co_2(OH)_{3.58}$-$(C_{22}H_{18}N_2O_6Co)_{0.21}$·$4H_2O$ (348.52): calcd. C 15.92, H 4.44, N 1.69, Co 37.37; found C 16.09, H 4.26, N 1.58, Co 36.84.

Cu–(*R*,*R*)-SCD–MnCl: The complex (*R*,*R*)-SCD-K_2–MnCl (0.32 g, 0.5 mmol) was suspended in water (50 mL). The pH of the solution was adjusted to 8 by using 0.2 M NaOH. Then $[Cu_2(OH)_3(DS)]$ (0.22 g, 0.48 mmol) was dispersed into the solution under an inert gas, and ethanol (50 mL) was added. The mixture was then stirred under argon at 80 °C for 24 h. After cooling to room temperature, a brown powder was isolated by filtration, washed with water and ethanol, and dried under vacuum. Yield: 60%. $Cu_2(OH)_{2.26}$-$(C_{22}H_{18}N_2O_6MnCl)_{0.87}$·$3H_2O$ (651.77): calcd. C 35.27, H 3.70, N 3.74, Cu 19.49, Mn 7.33; found C 35.22, H 4.07, N 3.53, Cu 19.44, Mn 7.33.

Cu–(*S*,*S*)-SCD–MnCl: The procedure was identical to that above, starting from (*S*,*S*)-SCD-K_2–MnCl. Yield: 60%. $Cu_2(OH)_{3.16}$-$(C_{22}H_{18}N_2O_6MnCl)_{0.42}$·$4.3H_2O$ (466.95): calcd. C 23.77, H 4.17, N 2.52, Cu 27.22, Mn 4.94; found C 23.92, H 3.97, N 2.77, Cu 27.12, Mn 4.86.

Cu–(*R*,*R*)-SCD–Co: The procedure was identical to that above, starting from (*R*,*R*)-SCD-K_2–Co. Yield: 53%. $Cu_2(OH)_{3.24}$-$(C_{22}H_{18}N_2O_6Co)_{0.30}(DS)_{0.16}$·$2.6H_2O$ (411.09):calcd. C 24.89, H 4.37, N 2.04, Cu 30.92, Co 4.30; found C 25.04, H 3.77, N 2.37, Cu 30.97, Co 3.54.

Cu–(*S*,*S*)-SCD–Co: The procedure was identical to that above, starting from (*S*,*S*)-SCD-K_2–Co. Yield: 45%. $Cu_2(OH)_{3.10}$-$(C_{22}H_{18}N_2O_6Co)_{0.45}$·$3.2H_2O$ (446.86): calcd. C 26.61, H 3.97, N 2.82, Cu 28.44, Co 5.93; found C 26.66, H 3.90, N 2.41, Cu 28.37, Co 6.16.

Synthesis of the Hybrid Materials M–SBD–M′ (M = Co, Cu; M′ = Mn, Co, "Al-Cl")

Co–SBD–AlCl: The complex SBD-H_2–AlCl (0.23 g, 0.5 mmol) was suspended in water (35 mL). The pH of the solution was adjusted to 8 by using 0.2 M NaOH. Then $[Co_2(OH)_3(DS_0)]$ (0.21 g, 0.48 mmol) was dispersed into the solution under an inert gas, and ethanol (35 mL) was added. The mixture was then stirred under argon at 80 °C for 15 h. After cooling to room temperature, an orange powder was isolated by filtration, washed with water and ethanol, and dried under vacuum. Yield: 48%. $Co_2(OH)_{2.94}$-$(C_{22}H_{12}N_2O_6AlCl)_{0.53}$·$4.5H_2O$ (494.20): calcd. C 28.34, H 3.73, N 3.00, Al 2.89, Co 23.84; found C 27.91, H 4.32, N 3.63, Al 2.89, Co 23.89.

Co–SBD–Co: The procedure was identical to that above, starting from SBD-H_2–Co. Yield: 50%. $Co_2(OH)_{2.84}(C_{22}H_{12}N_2O_6Co)_{0.58}$·$9H_2O$ (594.67): calcd. C 25.77, H 4.71, N 2.73, Co 25.57; found C 25.85, H 3.69, N 2.54, Co 26.24.

Co–SBD–MnCl: The procedure was identical to that above, starting from SBD-H_2–MnCl. Yield: 50%. $Co_2(OH)_{3.08}$-$(C_{22}H_{12}N_2O_6MnCl)_{0.46}$·$3.6H_2O$ (460.83): calcd. C 26.38, H 3.46, N

2.80, Mn 5.48, Co 25.58; found C 27.91, H 3.98, N 2.70, Mn 4.27, Co 25.53.

Cu–SBD–MnCl: The complex SBD-H_2–MnCl (0.25 g, 0.5 mmol) was suspended in water (50 mL). The pH of the solution was adjusted to 8 by using 0.2 M NaOH. Then $[Cu_2(OH)_3(DS)]$ (0.22 g, 0.48 mmol) was dispersed into the solution under an inert gas, and ethanol (50 mL) was added. The mixture was then stirred under argon at 80 °C for 15 h. After cooling to room temperature, a brown powder was isolated by filtration, washed with water and ethanol, and dried under vacuum. Yield: 50%. $Cu_2(OH)_{2.66}(C_{22}H_{12}N_2O_6MnCl)_{0.67}\cdot 2.6H_2O$ (547.96) calcd. C 32.31, H 2.92, N 3.43, Mn 6.72, Cu 23.19; found C 32.00, H 3.36, N 3.78, Mn 6.02, Cu 23.21.

Cu–SBD–Co: The procedure was identical to that above, starting from SBD-H_2–Co. Yield: 50%. $Cu_2(OH)_{2.84}(C_{22}H_{12}N_2O_6Co)_{0.58}\cdot 5.0H_2O$ (531.83): calcd. C 28.82, H 3.75, N 3.06, Co 6.42, Cu 23.89; found C 29.01, H 3.27, N 3.23, Co 7.21, Cu 23.51.

Supporting Information (see footnote on the first page of this article): FTIR spectra and list of absorption bands for all compounds, solid-state OCD spectra of (*R*,*R*)-SCD–MnCl and (*S*,*S*)-SCD–MnCl, magnetic measurements.

Acknowledgments

We thank the Centre National de la Recherche Scientifique (CNRS), the Université de Strasbourg, and the Agence Nationale de la Recherche (ANR contract 06-JCJC-0008 and 2010-BLAN-913-01 C-BLUE) for funding. S. E.-M. thanks the French Ministry for Education and Research for his Ph. D. grant. The authors thank C. Leuvrey and D. Burger for technical assistance, Dr. S. Bellemin-Laponnaz for tests of catalytic activity, and Drs. V. Béreau and J.-P. Sutter for helpful discussions.

---

[1] R. Andre, M. N. Tahir, F. Natalio, W. Tremel, *FEBS J.* **2012**, *279*, 1737–1749.

[2] M. Leskela, M. Ritala, O. Nilsen, *MRS Bull.* **2011**, *36*, 877–884.

[3] A. Winter, M. D. Hager, G. R. Newkome, U. S. Schubert, *Adv. Mater.* **2011**, *23*, 5728–5748.

[4] S. Gross, *J. Mater. Chem.* **2011**, *21*, 15853–15861.

[5] S. Minko, E. Katz, M. Motornov, I. Tokarev, M. Pita, *J. Comput. Theor. Nanosci.* **2011**, *8*, 356–364.

[6] B. Lebeau, P. Innocenzi, *Chem. Soc. Rev.* **2011**, *40*, 886–906.

[7] M. Barboiu, *Chem. Commun.* **2010**, *46*, 7466–7476.

[8] J. Le Bideau, L. Viau, A. Vioux, *Chem. Soc. Rev.* **2011**, *40*, 907–925.

[9] A. Leonard, P. Dandoy, E. Danloy, G. Leroux, C. F. Meunier, J. C. Rooke, B.-L. Su, *Chem. Soc. Rev.* **2011**, *40*, 860–885.

[10] M.-A. Neouze, *J. Mater. Chem.* **2010**, *20*, 9593–9607.

[11] E. Ruiz-Hitzky, K. Ariga, Y. Lvov, *Bio-inorganic Nanomaterials*, Wiley-VCH, Weinheim, **2008**.

[12] P. Gómez-Romero, C. Sanchez, *Functional Hybrid Materials*, Wiley-VCH, Weinheim, **2004**, .

[13] L. Nicole, L. Rozes, C. Sanchez, *Adv. Mater.* **2010**, *22*, 3208–3214.

[14] A. Mehdi, *J. Mater. Chem.* **2010**, *20*, 9281–9286.

[15] E. Ruiz-Hitzky, P. Aranda, M. Darder, G. Rytwo, *J. Mater. Chem.* **2010**, *20*, 9306–9321.

[16] S. Si, A. Taubert, A. Mantion, G. Rogez, P. Rabu, *Chem. Sci.* **2012**, *3*, 1945–1957.

[17] E. Coronado, J. R. Galán-Mascarós, C. J. Gómez-García, V. Laukhin, *Nature* **2000**, *408*, 447–449.

[18] E. Coronado, C. Martí-Gastaldo, E. Navarro-Moratalla, A. Ribera, S. J. Blundell, P. J. Baker, *Nat. Chem.* **2010**, *2*, 1031–1036.

[19] G. Rogez, C. Massobrio, P. Rabu, M. Drillon, *Chem. Soc. Rev.* **2011**, *40*, 1031–1058.

[20] S. Bhattacharjee, J. A. Anderson, *Chem. Commun.* **2004**, 554–555.

[21] P. Gomez-Romero, *Adv. Mater.* **2001**, *13*, 163–174.

[22] A. Illaik, C. Taviot-Guého, J. Lavis, S. Commereuc, V. Verney, F. Leroux, *Chem. Mater.* **2008**, *20*, 4854–4860.

[23] S. Bénard, A. Léaustic, E. Rivière, P. Yu, R. Clément, *Chem. Mater.* **2001**, *13*, 3709–3716.

[24] S. Benard, P. Yu, J. P. Audiere, E. Riviere, R. Clement, J. Guilhem, L. Tchertanov, K. Nakatani, *J. Am. Chem. Soc.* **2000**, *122*, 9444–9454.

[25] P. G. Lacroix, I. Malfant, S. Bénard, P. Yu, E. Rivière, K. Nakatani, *Chem. Mater.* **2001**, *13*, 441–449.

[26] K. Ladewig, Z. P. Xu, G. Q. Lu, *Expert Opin. Drug Delivery* **2009**, *6*, 907–922.

[27] J.-M. Oh, D.-H. Park, J.-H. Choy, *Chem. Soc. Rev.* **2011**, *40*, 583–595.

[28] B. Schwenzer, J. R. Neilson, K. Sivula, C. Woo, J. M. J. Fréchet, D. E. Morse, *Thin Solid Films* **2009**, *517*, 5722–5727.

[29] J.-M. Rueff, J.-F. Nierengarten, P. Gilliot, A. Demessence, O. Crégut, M. Drillon, P. Rabu, *Chem. Mater.* **2004**, *16*, 2933–2937.

[30] R. Ma, T. Sasaki, *Adv. Mater.* **2010**, *22*, 5082–5104.

[31] E. Delahaye, S. Eyele-Mezui, M. Diop, C. Leuvrey, P. Rabu, G. Rogez, *Dalton Trans.* **2010**, *39*, 10577–10580.

[32] E. Delahaye, S. Eyele-Mezui, M. Diop, C. Leuvrey, D. Foix, D. Gonbeau, P. Rabu, G. Rogez, *Eur. J. Inorg. Chem.* **2012**, 2731–2740.

[33] T. Yu, W. Su, W. Li, Z. Hong, R. Hua, B. Li, *Thin Solid Films* **2007**, *515*, 4080–4084.

[34] J. Xie, J. Qiao, L. Wang, J. Xie, Y. Qiu, *Inorg. Chim. Acta* **2005**, *358*, 4451–4458.

[35] P. G. Cozzi, L. S. Dolci, A. Garelli, M. Montalti, L. Prodi, N. Zaccheroni, *New J. Chem.* **2003**, *27*, 692–697.

[36] S. D. Bella, I. Fragala, I. Ledoux, T. J. Marks, *J. Am. Chem. Soc.* **1995**, *117*, 9481–9485.

[37] F. Averseng, P. G. Lacroix, I. Malfant, G. Lenoble, P. Cassoux, K. Nakatani, I. Maltey-Fanton, J. A. Delaire, A. Aukauloo, *Chem. Mater.* **1999**, *11*, 995–1002.

[38] P. G. Lacroix, *Eur. J. Inorg. Chem.* **2001**, 339–348.

[39] S. Di Bella, I. Fragala, I. Ledoux, M. A. Diaz-Garcia, T. J. Marks, *J. Am. Chem. Soc.* **1997**, *119*, 9550–9557.

[40] F. Averseng, P. G. Lacroix, I. Malfant, G. Lenoble, P. Cassoux, K. Nakatani, I. Maltey-Fanton, J. A. Delaire, A. Aukauloo, *Chem. Mater.* **1999**, *11*, 995–1002.

[41] M. R. Ganjali, M. R. Pourjavid, M. Rezapour, T. Poursaberi, A. Daftari, M. Salavati-Niasari, *Electroanalysis* **2004**, *16*, 922–927.

[42] V. K. Gupta, R. N. Goyal, A. K. Jain, R. A. Sharma, *Electrochim. Acta* **2009**, *54*, 3218–3224.

[43] E. N. Jacobsen, W. Zhang, A. R. Muci, J. R. Ecker, L. Deng, *J. Am. Chem. Soc.* **1991**, *113*, 7063–7064.

[44] A. M. Jason, J. Wiechang, T. N. SonBinh, *Angew. Chem.* **2002**, *114*, 3077; *Angew. Chem. Int. Ed.* **2002**, *41*, 2953–2956.

[45] M. G. Gichinga, S. Striegler, N. A. Dunaway, J. D. Barnett, *Polymer* **2010**, *51*, 606–615.

[46] H. Zhang, Y. Zhang, C. Li, *Chem. Commun.* **2005** 1209–1211.

[47] G. Wu, X. Wang, J. Li, N. Zhao, W. Wei, Y. Sun, *Catal. Today* **2008**, *131*, 402–407.

[48] V. Béreau, V. Jubera, P. Arnaud, A. Kaiba, P. Guionneau, J.-P. Sutter, *Dalton Trans.* **2010**, *39*, 2070–2077.

[49] S. N. Poddar, *Z. Anorg. Allg. Chem.* **1963**, *322*, 326–336.

[50] R. Kitaura, G. Onoyama, H. Sakamoto, R. Matsuda, S.-i. Noro, S. Kitagawa, *Angew. Chem.* **2004**, *116*, 2738; *Angew. Chem. Int. Ed.* **2004**, *43*, 2684–2687.

[51] Y.-M. Jeon, J. Heo, C. A. Mirkin, *Tetrahedron Lett.* **2007**, *48*, 2591–2595.

[52] F. Gasbøl, P. Steenbøl, B. S. Sørensen, *Acta Chem. Scand.* **1972**, *26*, 3605–3611.

[53] J. F. Larrow, E. N. Jacobsen, C. H. Senanayake, J. Liu, I. Shinkai, *Org. Synth. Coll. Vol.* **2004**, *10*, 96.
[54] J. Hanson, *J. Chem. Educ.* **2001**, *78*, 1266–1268.
[55] W. Nowicki, *Transition Met. Chem.* **1996**, *21*, 469–471.
[56] E. Delahaye, S. Eyele-Mezui, J.-F. Bardeau, C. Leuvrey, L. Mager, P. Rabu, G. Rogez, *J. Mater. Chem.* **2009**, *19*, 6106–6115.
[57] V. Laget, C. Hornick, P. Rabu, M. Drillon, R. Ziessel, *Coord. Chem. Rev.* **1998**, *178–180*, 1533–1553.
[58] V. Laget in *Matériaux magnétiques hybrides: Influence d'espaceurs organiques et de radicaux dans des sels basiques lamellaires de cuivre et de cobalt*, Ph.D. thesis, Université Louis Pasteur, Strasbourg, **1998**.
[59] M. Louër, D. Louër, D. Grandjean, *Acta Crystallogr., Sect. B* **1973**, *29*, 1696–1703.
[60] M. Kurmoo, *Phil. Trans. R. Soc. London A* **1999**, *357*, 3041–3061.
[61] W. Fujita, K. Awaga, *Inorg. Chem.* **1996**, *35*, 1915–1917.
[62] S. P. Newman, W. Jones, *J. Solid State Chem.* **1999**, *148*, 26–40.
[63] V. Laget, C. Hornick, P. Rabu, M. Drillon, *J. Mater. Chem.* **1999**, *9*, 169–174.
[64] S. Yamanaka, T. Sako, K. Seki, M. Hattori, *Solid State Ionics* **1992**, *53–56*, 527–533.
[65] S. H. Park, C. H. Lee, C. E. Lee, H. C. Ri, S. Y. Shim, *Mater. Res. Bull.* **2002**, *37*, 1773–1779.
[66] S.-H. Park, C. E. Lee, *J. Phys. Chem. B* **2005**, *109*, 1118–1124.
[67] W. Fujita, K. Awaga, T. Yokoyama, *Inorg. Chem.* **1997**, *36*, 196–199.
[68] N. Masciocchi, E. Corradi, A. Sironi, G. Moretti, G. Minelli, P. Porta, *J. Solid State Chem.* **1997**, *131*, 252–262.
[69] S. Švarcová, M. Klementová, P. Bezdička, W. Łasocha, M. Dušek, D. Hradil, *Cryst. Res. Technol.* **2011**, *46*, 1051–1057.
[70] N. S. Youssef, E. El-Zahany, A. M. A. El-Seidy, A. Caselli, S. Fantauzzi, S. Cenini, *Inorg. Chim. Acta* **2009**, *362*, 2006–2014.
[71] H. Liu, H. Wang, D. Niu, Z. Lu, *Synth. React. Inorg., Met.-Org., Nano-Met. Chem.* **2005**, *35*, 779–783.
[72] M. R. Maurya, C. Haldar, A. A. Khan, A. Azam, A. Salahuddin, A. Kumar, J. Costa Pessoa, *Eur. J. Inorg. Chem.* **2012**, 2560–2577.
[73] A. Emara, O. Adly, *Transition Met. Chem.* **2007**, *32*, 889–901.
[74] A. A. Soliman, W. Linert, *Thermochim. Acta* **1999**, *338*, 67–75.
[75] N. Raman, Y. P. Raja, A. Kulandaisamy, *Proc. Indian Acad. Sci., Chem. Sci.* **2001**, *113*, 183–189.
[76] J. W. Ledbetter, *J. Phys. Chem.* **1977**, *81*, 54–59.
[77] C. Jin, Y. J. Jia, B. B. Fan, J. H. Ma, R. F. Li, *Chin. Chem. Lett.* **2006**, *17*, 419–422.
[78] C. Dendrinou-Samara, G. Tsotsou, L. V. Ekateriniadou, A. H. Kortsaris, C. P. Raptopoulou, A. Terzis, D. A. Kyriakidis, D. P. Kessissoglou, *J. Inorg. Biochem.* **1998**, *71*, 171–179.
[79] K. Nakamoto, *Infrared and Raman Spectra of Inorganic and Coordination Compounds*, 4th ed., Wiley Interscience, New York, **1986**.
[80] M. Salavati-Niasari, Z. Salimi, M. Bazarganipour, F. Davar, *Inorg. Chim. Acta* **2009**, *362*, 3715–3724.
[81] B. Bosnich, *J. Am. Chem. Soc.* **1968**, *90*, 627–632.
[82] A. B. P. Lever, *Inorganic Electronic Spectroscopy*, 2nd ed., Elsevier, Amsterdam, **1984**, .
[83] A. Demessence, G. Rogez, P. Rabu, *Chem. Mater.* **2006**, *18*, 3005–3015.
[84] R. L. Carlin, *Magnetochemistry*, Springer, Berlin, **1986**, p. 328.
[85] Y.-M. Legrand, A. van der Lee, N. Masquelez, P. Rabu, M. Barboiu, *Inorg. Chem.* **2007**, *46*, 9083–9089.
[86] É. Delahaye, M. Diop, R. Welter, M. Boero, C. Massobrio, P. Rabu, G. Rogez, *Eur. J. Inorg. Chem.* **2010**, 4450–4461.
[87] Y. Ma, N. A. G. Bandeira, V. Robert, E.-Q. Gao, *Chem. Eur. J.* **2011**, *17*, 1988–1998.
[88] Y.-T. Li, C.-W. Yan, Y.-F. Lu, D.-Z. Liao, *Transition Met. Chem.* **1998**, *23*, 237–240.
[89] A. Demessence, A. Yassar, G. Rogez, L. Miozzo, S. De Brion, P. Rabu, *J. Mater. Chem.* **2010**, *20*, 9401–9414.

Received: June 25, 2012

Functionalized Layered Hybrids

New hybrid layered simple hydroxides have been obtained by the functionalization of cobalt and copper hydroxides by carboxy-salen-type complexes.

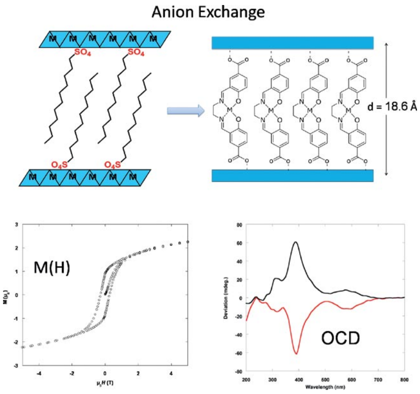

S. Eyele-Mezui, E. Delahaye, G. Rogez,* P. Rabu* **1–15**

Functional Hybrid Materials Based on Layered Simple Hydroxide Hosts and Dicarboxylate Schiff Base Metal Complex Guests

Keywords: Hybrid materials / Layered compounds / Schiff bases / Magnetic properties / Hydroxides